Fiber optic sensor for distributed liquid content quantification in subsurface

S. Texier & S. Pamukcu
Lehigh University, Bethlehem, Pennsylvania, USA

ABSTRACT: A novel fiber-optic sensor assembly for continuous monitoring of moisture over extended subsurface environments, such as road embankments, wall backfills, and landfills is presented. This sensor meets the requirements of subsurface monitoring by distributed measurements over linear positioning of a single fiber. The sensor assembly is composed of a communication optical fiber and a hydrophilic polymer. A phenomena associated with the backscattering of light, namely Brillouin scattering, correlates to the velocity of acoustic wave within the fiber, and in turn its elastic response. A hydrophilic polymer is coupled with the optical fiber at discrete locations along the fiber. Upon exposure to moisture, the swelling polymer exerts stress on the fiber. The resulting Brillouin shift response is then calibrated to determine the moisture level in the surrounding environment.

1 INTRODUCTION

1.1 Types of optical sensing

Fiber Bragg Gratings, (FBG), Optical Time Domain Reflectometry (OTDR), evanescent pulse technique and, nonlinear techniques such as Raman and Brillouin scattering are among the various types of optical sensing. FBG technique uses the marking of a fiber with a high power laser in order to create a local narrow bandpass filter. The bandpass region becomes the sensor, reacting to environmental parameters such as strain and temperature. OTDR consists of sending a powerful light pulse in the waveguide and observe the changes in the reflected light due to local inhomogeneities along the fiber. The pulse losses correspond to specific interactions between the surrounding environment and the fiber. In evanescent pulse technique, which is also based on OTDR, the fiber cladding is modified in order to interact with specific environmental compounds such as pollutants. All of these sensors are based on "interaction/loss" type of detection. They demand large optical power due to loss of the cumulative energy at the points of contact with the environment (i.e. chemical). Hence, frequent encounters with the sensed condition give rise to complete power loss over extended distances. Alternatively, there are optical sensors based on nonlinear effects such as Raman and Brillouin phenomena. These sensors are not based on "interaction/loss" type of detection, therefore may present advantages for long term health monitoring of civil infrastructure. They are truly distributed, and efficient over very long distances. Data acquisition and conditioning systems can be elaborate and costly but they have been demonstrated to be very accurate.

1.2 Brillouin sensing

The premise of this technique goes back to 1920 when Léon Brillouin (1889-1969), first studied the diffusion of light by acoustic waves. The first series of major papers on distributed fiber optic sensor based on *Brillouin scattering* came in the mid-nineties [Bao et al., 1995; Garus et al, 1995; Nikles et al, 1996; Czarske, 1996]. Some features of the technique, such as the distributive measurement aspect, drift free, high strain resolution and

1

calibration free application led to considerable interest in the civil engineering community [Jackson, 1995; Kurashima et al., 1997; Czarske et al., 1996; Culshaw & Michie, 1997]. Thevenaz et al. in 1999 reported the first full-scale application of a Brillouin scattering sensor. In this study, they implemented the sensor into a concrete dam structure. They measured the concrete curing temperature distribution over 72 hours. Since, the sensor has been used successfully for measuring compressive, tensile, and flexural strains in structural components [Bao et al., 2001a, b; Kim et al., 2002; Zeng et al., 2002]; temperatures during construction of buildings [Kwon et al, 2002]; and strains in concrete piles [Ohno et al., 2002].

1.3   *Physics of Brillouin scattering*

When light travels through a transparent media, part of it is scattered. This phenomenon is related to the in-homogeneities in the material structure. In a dielectric material like the silica of an optical fiber, material tends to densify in the regions of high intensity electrical field (electrostriction), as sketched in Figure 1.
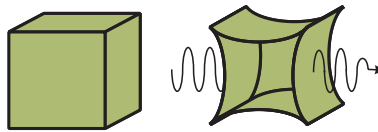

Figure 1. Electrostriction in a dielectric material

Hence, periodic compression zones create a density wave moving in the material. If the speed of this wave corresponds to the speed of sound in the material, an acoustic wave is created. Brillouin Scattering results from the scattering of the incident light by these acoustic waves. The scattered light is shifted downward in frequency to the Stokes frequency. The frequency shift of the Stokes waves, referred to as the Brillouin frequency shift, ν_B is then given by the following equation:

$$\nu_B = \omega_p - \omega_S / 2\pi = 2nV_a/\lambda_p \qquad (1)$$

where ω_p and ω_S are the frequencies of the pump and the Stokes waves, λ_p, n and V_a are the wavelength of the incident pump, the refractive index of the fiber core and the acoustic velocity of the material, respectively. According to Eq.(1), the Brillouin frequency shift is directly proportional to the acoustic velocity, so that any change of this velocity results in a shift of the ν_B. The elastic properties of silica make any induced strain a volume change, resulting in locally modified material density. When the refractive index, n, of the fiber is known, by measuring the Brillouin shift ν_B, one can determine the local change in the acoustic velocity and the induced strain [Horigushi et al., 1989]. Hence, by determining the proportionality constant between the two quantities, one can obtain the strains corresponding to ν_B values measured at discrete points along the fiber. This makes Brillouin sensing a very efficient tool for strain monitoring.

2   WATER CONTENT SENSOR

2.1   *Development of the photonic setup*

The signal processing assembly is shown in Figure 2. This setup requires two diode lasers and the use of an electro-optical modulator (EOM) device through which the continuous wave light can be modified as a pulsed light. Measurements are based on the interaction of the two counter-propagating light beams in fiber. A pulsed pump laser beam launched into the fiber interacts with a counter-propagating continuous wave (cw) laser beam at a higher frequency. At a particular location where the beat frequency between these laser beams is within the Brillouin loss profile of the fiber, some power is transferred from the pulse to the cw through the Brillouin loss mechanism. If the cw power is monitored in the time domain, Brillouin loss will manifest itself as a measurable gain in the cw signal at a particular time

corresponding to twice the time for the pulse to travel to and from that particular position. By scanning a range of beat frequencies and measuring the gain of power for each one, the entire Brillouin Loss Spectra (BLS) can be determined at discrete locations on the fiber. The ν_B is the center frequency of the BLS.
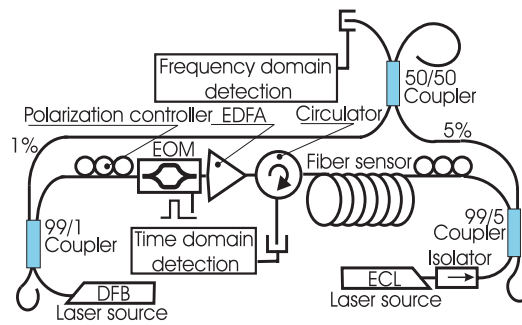

Figure 2. Counter-propagating light setup

2.2 *Development of the transducer*

A hydrophilic polymer was coupled to the optical fiber, such that the fiber is stretched as the polymer swell in water. Several polymers and different geometric designs were tested to develop a suitable water transducer. A workable transducer configuration achieved is shown in Figure 3. A 3-cm diameter polymer rod was drilled in the middle to fit a 1.3-cm diameter rigid acrylic rod. The acrylic rod was used to limit the volumetric expansion and to shorten the swelling and drying times by reducing the radial diffusion distance. In the final design, each water transducer was a 3-cm long, 3-cm diameter cylinder with 2-meter fiber wound and secured over the drum. This configuration was selected to maximize stress transfer between fiber and polymer, and also to reduce the physical length of the sensor. Hence, numerous sensors, of few centimeters in length can be hitched at intervals of one meter or less on a single continuous fiber.
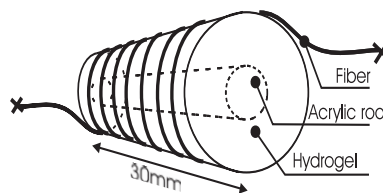

Figure 3. Water content transducer

In polymer selection, the consistency of the wet polymer was considered to avoid taught fiber cut into the softened material. The kinetics of expansion, reversibility and mechanical stability are also critical characteristics that ought to be investigated and optimized for the final design. These characteristics, however, were not investigated for the initial design, which was aimed to demonstrate the concept in this work. The hydrogel selected was a solid rod of pure hydrophilic polymer (AEP 80 series - Table 1) obtained from IHP Polymers Inc. in UK. It is a cross-linked polymer with good mechanical stability and accurate expansion characteristics. Full expansion is reproducible over many wetting and drying cycles and is consistent over a wide range of pH and dissolved solid concentrations.

The water reactivity and linearity of the polymer rods were tested using a simple scheme. Four transducers of each type, were embedded in acrylic cells containing medium Ottawa sand of 4 different water contents. The watertight cells, 7 cm in diameter and 14 cm high, were completely filled with wet compacted sand. The transducers were embedded at the center of each cell and left to equilibrate for 5 days, turning over every 6 hrs to avoid segregation. After 5 days, the polymer water-contents were measured and compared with the initial soil water-contents, as shown in Figure 4. A linear trend was observed for both polymer types, with AEP 80 displaying a larger mass gain.

3

Table 1. Polymer characteristics

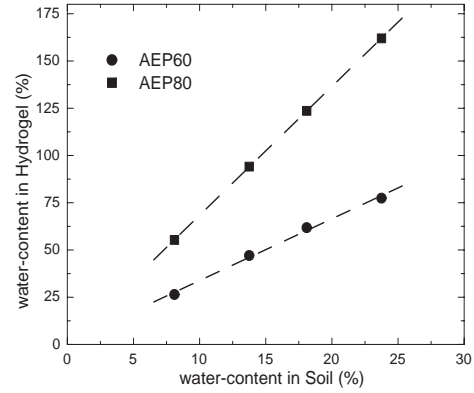| Polymer type	Volume expansion %	Hydrated tensile modulus MPa
AEP 80	557	0.35
AEP 60	227	0.45

Figure 4. Equilibrium water-contents of the 2 polymers after 5 days in a sealed soil cells

3   TEST RESULTS

3.1   Strain Calibration

The local strain vs. Brillouin shift relationship of the Truewave™ fiber was established using a 3-pulley system. A 69-meter long spool of optic fiber was hooked to the pulley assembly, with only an arbitrary 2-meter section strained using calibrated weights. When the local Brillouin shift at the position of sensing corresponded to the frequency shift between pump and probe lasers, one could clearly observe a gain in the probe at that location. Figure 5 shows a trace of this sweep on the oscilloscope record. The peak observed at 20.8 meters corresponds to the exact location where the fiber is stretched using a calibrated weight.

Knowing the elastic constants and the cross-sectional area of the fiber, the strain amplitudes could be computed. Figure 6 shows the best linear fit to the strain data set obtained. Since the frequency adjustment was done manually in this particular set up, accuracy and linearity may be compromised due to operator bias. The next generation of photonics set up will eliminate operator bias through automated frequency adjustment, hence should deliver higher accuracy in measurements.

3.2   Water content calibration

Three water content transducers were hitched on a 100-meter fiber, each separated by 10 meters of fiber. The three sensors were immersed in water at 25°C simultaneously. The polymers absorbed water and expanded radially, stretching the wound fiber on the periphery. Figure 7 shows a record of the probe gains on digital oscilloscope at the positions of the three sensors after 2188 minutes of soaking.

The Brillouin shift at the sensor locations evolved with time since the rate of strain is controlled by the rate of water diffusion into the polymer. Once the Brillouin measurements showed no change in swelling, the three sensors were removed from the beakers and left to dry at 25°C. The Brillouin measurements were continued during the drying phase also. As the Brillouin shift was measured in time, the corresponding polymer masses were also recorded at those same times. Figure 8 shows the evolution of water mass gain (as percentage of initial mass) and the corresponding Brillouin shift with time in one of the transducers. It is observed that the Brillouin shift, ν_B, reached a maximum of 10.892GHz after 1190 minutes of soaking at which, the polymer water content is 32%. The water-content in the hydrogel, however, kept increasing for the next two data intervals while the ν_B remained constant. A closer look at the transducers and the trend of the data suggested that, the wound fiber stretched to a limit where the radial component of the axial stress in the fiber was large enough to exert an equilibrating confinement to the radial swelling of the polymer rod. The swelling, however, continued longitudinally at the ends of the rod, which ultimately resulted in a distorted shape, with bulging ends and a restrained central section.
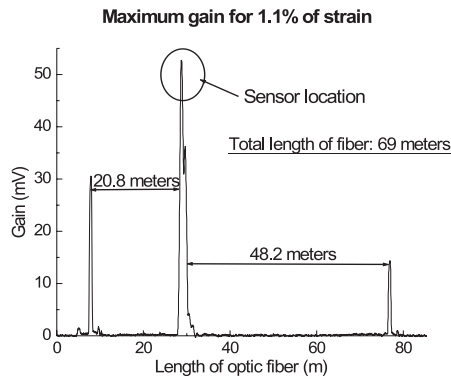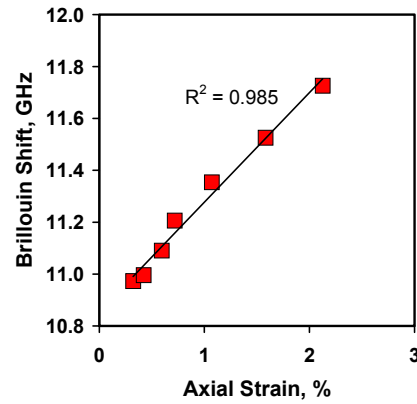
Figure 5. Probe gain signal for local strain

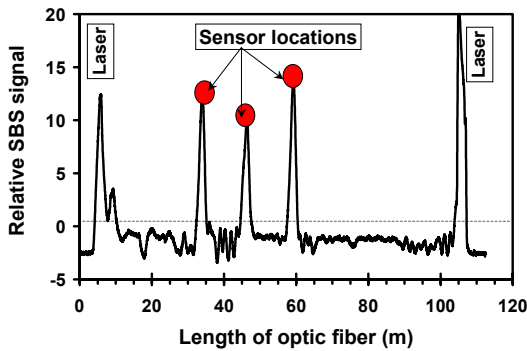Figure 6. Fiber calibration for strain

Figure 7. Maximum probe gain for the three sensors after 2188 minutes of soaking
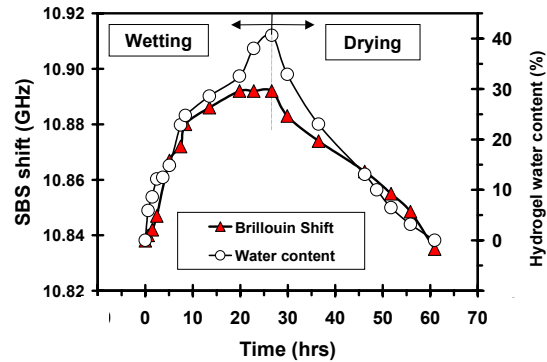

Figure 8. Evolution of the water-content in the transducers and Brillouin shift with time

When the three sensors were set to dry, the Brillouin shift measurements followed the drying phase as it decreased back to the initial values. Comparing the Brillouin shift evolution of the wetting phase and the drying phase, one observes the presence of a hysteresis as plotted in Figure 9. The hysteresis behavior is attributed to the physical shape and the configuration of the transducer as well as the swelling and shrinkage kinetics of the polymer. During swelling, the rate of diffusion of the liquid into the polymer and the increasing confining of the fiber govern the evolution of the Brillouin shift. The drying phase shows a different behavior because the rate of diffusion of the liquid out of the polymer is not uniform over the entire surface of the transducer owing to its final distorted shape. Therefore, the observed Brillouin shift decreases faster compared to the real water content of the polymer.
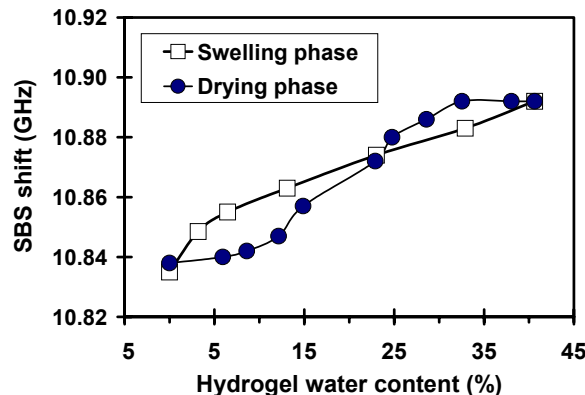

Figure 9. Comparison of the Brillouin shift evolution between wetting and drying phases

5

4   CONCLUSIONS

In conclusion, these results demonstrated the effective use of Brillouin scattering principles for liquid content measurement in soils. The technology can be applied to not only measurement of water content, but also other liquid contents for environmental applications. The next generation of polymer coupled optical fiber sensors are envisioned with a simpler geometry and well defined swelling-shrinkage kinetics that should lend itself to use in embedding media, on surfaces and in water reservoirs to detect trace amounts of contaminants on-line and in distributed manner.

5   ACKNOWLEDGMENTS

6   REFERENCES

Bao, X., M. DeMerchant, A. Brown, and T. Bremmer. 2001a. Strain measurement of the steel beam with the distributed Brillouin scattering sensor. In *Proceedings of SPIE - The International Society for Optical Engineering*, 4337: 223.

Bao, X., M. DeMerchant, A. Brown, and T. Bremner. 2001b. Tensile and compressive strain measurement in the lab and field with the distributed Brillouin scattering sensor. *Journal of Lightwave Technology*, 19:1698.

Bao, X., J. Dhliwayo, N. Heron, D.J. Webb, and D.A. Jackson. 1995. Experimental and theoretical studies on a distributed temperature sensor based on Brillouin scattering. *Journal of Lightwave Technology*, 13:1340.

Culshaw, B., and W.C. Michie. 1997. Optical fiber sensors and their role in smart structures. In *Proceedings of the SPIE - The International Society for Optical Engineering*, 3211:432.

Czarske, J.W., 1996. Simplified distributed temperature sensor using stimulated Brillouin scattering. In *International Conference on Optical Fiber Sensors*, pp514.

Czarske, J.W., I. Freitag, and A. Tuennermann. 1996. Novel concepts of distributed temperature fiber sensors based on Brillouin scattering. In *Conference on Lasers and Electro-Optics Europe - Technical Digest*, p193.

Garus, D., K. Krebber, and R. Hereth. 1995. Distributed fiber optical sensors using Brillouin backscattering. In *Proceedings of the SPIE - The International Society for Optical Engineering*, 2510:172.

Horigushi, T., T. Kurashima, and M. Tateda. 1989. Dependence of Brillouin frequency shift in silica optical fibers. *IEEE photon. Technol. Lett.*, 1:107.

Jackson, D.A., 1995. Potential of fiber optic point and distributed fiber optic sensors for structural monitoring. In *IEEE Colloquium (Digest)*, pp 4/1.

Kim, S.H., Jung-Ju Lee, and Il-Bum Kwon. 2002. Structural monitoring of a bending beam using Brillouin distributed optical fiber sensors. *Smart Materials and Structures*, 11:396.

Kurashima, T., T. Usu, K. Tanaka, A. Nobiki, M. Sato, and K. Nakai. 1997. Application of fiber optic distributed sensor for strain measurement in civil engineering. In *Proceedings of the SPIE - The International Society for Optical Engineering*, 3241: 247.

Kwon,I.B., C.Y. Kim, and M.Y. Choi. 2002. Continuous measurement of temperature distributed on a building construction. In *Proceedings of SPIE - The International Society for Optical Engineering*, 4696: 273.

Nikles, M., L. Thevenaz, and P.A. Robert. 1996. Simple distributed fiber sensor based on Brillouin gain spectrum analysis. *Optics Letters*, 21:758.

Ohno, H. Hiroshi Naruse, Toshio Kurashima, Atsushi Nobiki, Yasuomi Uchiyama, and Yuki Kusakabe. 2002. Application of Brillouin scattering-based distributed optical fiber strain sensor to actual concrete piles. *IEICE Transactions on Electronics*, E85-C:945.

Thevenaz, L., Massimo Facchini, Alexandre Fellay, Philippe Robert, Daniele Inaudi, and Boris Dardel. 1999. Monitoring of large structure using distributed Brillouin fiber sensing. *Proceedings of SPIE - The International Society for Optical Engineering*, 3746:345.

Zeng, X., Xiaoyi Bao, Chia Yee Chhoa, T.W. Bremner, A.W. Brown, M.D. DeMerchant, G. Ferrier, A.L. Kalamkarov, and A.V. Georgiades. 2002. Strain measurement in a concrete beam by use of the Brillouin-scattering-based distributed fiber sensor with single-mode fibers embedded in glass fiber reinforced polymer rods and bonded to steel reinforcing bars. *Applied Optics*, 41:5105.